Formation of OX-1R/CB$_1$R heteromeric complexes in embryonic mouse hypothalamic cells: Effect on intracellular calcium, 2-arachidonoyl-glycerol biosynthesis and ERK phosphorylation

Roberta Imperatore [a], Letizia Palomba [b], Giovanna Morello [a], Alessandro Di Spiezio [c], Fabiana Piscitelli [a], Vincenzo Di Marzo [a], Luigia Cristino [a,*]

[a] Endocannabinoid Research Group, Institute of Biomolecular Chemistry, Consiglio Nazionale delle Ricerche, Pozzuoli, Italy
[b] Department of Biomolecular Sciences, University of Urbino "Carlo Bo", Urbino, Italy
[c] Institute of Experimental and Clinical Pharmacology and Toxicology, University of Luebeck, Luebeck, Germany

ARTICLE INFO

ABSTRACT

Orexin 1 (OX-1R) and cannabinoid receptor (CB$_1$R) belong to the superfamily of G-protein-coupled receptors (GPCRs) and are mostly coupled to Gq and Gi/o proteins, respectively. In vitro studies in host cells over-expressing OX-1R and CB$_1$R revealed a functional interaction between these receptors, through either their ability to form heteromers or the property for OX-1R to trigger the biosynthesis of 2-arachidonoylglycerol (2-AG), an endogenous CB$_1$R ligand. Since: i) OX-1R and CB$_1$R co-espression has been described at postsynaptc sites in hypothalamic circuits involved the regulation of energy homeostasis, and ii) increased orexin-A (OX-A) and 2-AG levels occur in hypothalamic neurons during obesity, we sought here to investigate the OX-1R/CB$_1$R interaction in embryonic mouse hypothalamic NPY/AgRP mHypoE-N41 neurons which express, constitutively, both receptors. Treatment of mHypoE-N41 cells with OX-A (0.1-0.3 μM), but not with the selective CB$_1$R agonist, arachidonyl-2-chloroethylamide (ACEA; 0.1-0.3 μM), transiently elevated [Ca^{2+}]$_i$. Incubation with a subeffective dose of OX-A (0.1 μM) + ACEA (0.1 μM) led to stronger and longer lasting elevation of [Ca^{2+}]$_i$, antagonized by OX-1R or CB$_1$R antagonism with SB-334867 or AM251, respectively. FRET and co-immunoprecipitation experiments showed the formation of OX-1R/CB$_1$R heteromers after incubation with OX-A (0.2 μM), or OX-A (0.1 μM) + ACEA (0.1 μM), but not after ACEA (0.2 μM), in a manner antagonized by SB-334867 or AM251. OX-A (0.2 μM) or OX-A (0.1 μM) + ACEA (0.1 μM) also led to 2-AG biosynthesis. Finally, a stronger activation of ERK1/2$^{Thr202/185}$ phosphorylation in comparison to basal or each agonist alone (0.1-0.2 μM), was induced by incubation with OX-A (0.1 μM) + ACEA (0.1 μM), again in a manner prevented by OX-1R or CB$_1$R antagonism. We suggest that OX-A, alone at effective concentrations on [Ca^{2+}]$_i$, or in combination with ACEA, at subeffective concentrations, triggers intracellular signaling events via the formation of OX-1R/CB$_1$R heteromers and an autocrine loop mediated by 2-AG.

© 2016 Elsevier Ltd. All rights reserved.

1. Introduction

The cannabinoid receptor of type 1 (CB$_1$R) belongs to the family of G-protein-coupled receptors (GPCRs). It is mainly coupled to Gi, through which it stimulates mitogen-activated kinases and inhibits N-, P/Q- and L-type Ca^{2+} channels as well as adenylyl cyclase (AC) activity, with downstream activation of A-type K+ channels [1]. Receptors for orexin-A (OX-1R) or orexin-B (OX-2R) are GPCRs belonging to the rhodopsin family [2]. OX-2R couples to the G$_q$, G$_s$ or G$_{i/o}$ subclasses of G proteins and exhibits equal affinity for OX-A and OX-B [3]. OX-1 R is mostly coupled to G$_q$ [2] and is activated 10 times more potently by OX-A than OX-B. Both OX-A and OX-B are produced by enzymatic cleavage of the prepro-orexin (PPO), whose expression is restricted to a small number of neuronal cell bodies in the lateral hypothalamus (LH) [2,4,5]. OX-A is a 33-amino acid peptide of 3562 Da [2] and OX-B is a 28-amino acid of 2937 Da sharing 46% sequence homology with OX-A. Since OX-A and OX-B

are very ancient neuromodulators, their amino acid sequences are characterized by strong phylogenetic conservation [6,7].

In 2003, Hilairet et al. reported for the first time the incidence of heteromultimerization between CB_1R and OX-1R in Chinese hamster ovary (CHO) cells stably co-transfected with the cDNAs encoding for these receptors. Notably, heterologous CB_1R and OX-1R co-expression improved OX-A-mediated ERK1/2 stimulation up to ~100-fold more than when only one of the receptors was expressed in cells [8]. This evidence was further demonstrated by electron microscopy in OX-1R and CB_1R co-transfected HEK293 cells [9] and by fluorescence resonance energy transfer and co-immunoprecipitation of receptors tagged, respectively, by "SNAP" and "CLIP" labeling at extracellular domain in Flp-In T-REx 293 cells [10].

Besides heteromerization, the potenziation of ERK1/2 phosphorylation was attributed to the strong enhancement of the production of the endogenous agonist of CB_1R, 2-arachidonoylglycerol (2-AG), triggered by the activation of Gq-PLCβ-DAGLα pathway [3,11,12]. Several studies have confirmed the ability of OX-A to potentiate CB_1R signaling in vivo, pointing to the functional effect of this interaction in the regulation of appetite, nociception, and anxiety-like behaviors because of the widespread co-expression of these receptors in different regions of the brain, including the periaqueductal gray (PAG) [13,14], LH [15], ventral tegmental area [16] and arcuate nucleus of the hypothalamus [17]. Taking into account that: i) OX-1R and CB_1R co-expression occurs at postsynaptic sites in the hypothalamic circuits regulating energy homeostasis [17], and ii) hypothalamic OX-A and 2-AG levels increase during obesity [15,18], the aim of this study was to investigate whether the embryonic mouse immortalized hypothalamic cell line (mHypoE-N41) constitutively express both OX-1R and CB_1R and can be used as an easily available in vitro model for the study of OX-1R and CB_1R interactions. Since NPY/AgRP is the main signaling system in mHypoE-N41 cells, these neurons also represent an in vitro model for the study of the regulation of the orexigenic pathways of the ARC.

We investigated OX-1R – CB_1R heteromerization, and its consequences on the Gq(OX-1R)-PLC-DAGLα-2-AG pathway, $[Ca^{2+}]_i$ and downstream phosphorylation of ERK1/2$^{Thr202/185}$ by means of calcium imaging, FRET and co-immunoprecipitation experiments and of 2-AG quantification by liquid chromatography-mass spectrometry (LC–MS) in mHypoE-N41 cells.

2. Materials and methods

2.1. Chemicals

OX-A, arachidonyl-2′-chloroethylamide (ACEA), 1-[2-methylbenzoxazol-6-yl]-3-[1,5]naphthyridin-4-yl-urea HCl (SB-334867) and 1-(2,4-dichlorophenyl)-5-(4-iodophenyl)-4-methyl-N-1-piperidinyl-1H-pyrazole-3-carboxamide (AM251) as well as most reagent-grade chemicals were purchased from Tocris Bioscience (Bristol, UK).

2.2. Cell culture

mHypoE-N41cells were cultured in Dulbecco's modified Eagle's medium (Life Technologies) supplemented with 10% fetal bovine serum (Life Technologies), penicillin (50 units/ml) and streptomycin (50 μg/ml), at 37 °C in 100 mm culture dishes (Life Technologies) gassed with an atmosphere of 95% air-5% CO2.

2.3. Immunocytochemical analysis

mHypoE-N41cells were seeded on polylysine-coated coverslips, washed with PBS and fixed 20 min with paraformaldehyde 4% in phosphate buffer pH 7.4, 0.1 M. The cells were then rinsed with PB and incubated for 30 min in normal donkey serum (NDS; Jackson Immunoresearch) 10% in phosphate buffer pH 7.4, 0.1 M and finally incubated 4 h at room temperature in a mixture of rabbit anti-CB_1R (dilution 1:200, Calbiochem) and goat anti-OX-1R (dilution 1:100, Santa Cruz). After, the cells were washed and incubated 2 h in the appropriate mixture of fluorochrome-conjugated secondary antibodies (donkey anti-goat Alexa Fluor 488 and donkey anti-rabbit Alexa Fluor 594, diluited 1:50 in NDS block solution) and finally counterstained with DAPI (4′,6-diamidino-2-phenylindole). The cells were observed with a Leica DMI6000 fluorescence microscope equipped with a Leica DFC360 cooled digital CCD camera (Leica Microsystems) and the images were analyzed by LAS AF 2.2.0 software. The specificity of the antibody for OX-1R was tested in Hcrtr1 (gene encoding OX-1R)-silenced mHypoE-N41 cells by using western blot analysis.

2.4. Hcrtr1 gene silencing

The Hcrtr1 gene was silenced by transfecting mHypoE-N41 cells with endoribonuclease-prepared siRNA sequences (sc-36131; Santa Cruz Biotechnology) using Lipofectamine 2000 (Life Tecnologies) according to the manufacturer's instructions. The siRNA silencing efficiency was determined 48 h after the initial transfection by measuring the relative amount of OX-1R protein by western blot analysis (see above).

2.5. Calcium imaging

$[Ca^{2+}]_i$ was assayed using a cell-permeable Ca^{2+} indicator, Fluo-4AM (Life Technologies), dissolved in DMSO containing 0.02% pluronic F-127 (Life Technologies). Briefly, the cells, seeded on polylysine-coated coverslips, were loaded with 1 μM Fluo-4AM (20 min) in serum free medium. The coverslips were placed into a perfusion chamber (Leica Microsystems GmbH, Wetzlar, Germany) mounted on the stage of a Leica digital microscope DMI6000 equipped with CO_2 incubator cage (OkoLab, Burlingame, USA) providing saturated humidity atmosphere containing 95% air and 5% CO_2 at 37 °C. For calcium recording, the cells were incubated in the extracellular solution (145 mM NaCl, 2.5 mM KCl, 1.5 mM $CaCl_2$, 1.2 mM $MgCl_2$, 10 mM D-glucose, and 10 mM HEPES, pH 7.4) and perfused with each drug dissolved in the same solution. All the observations and acquisitions of images were performed with 20X objective lens and carried out by appropriate filter. The excitation and emission wavelengths for Fluo-4AM were 460–495 nm and 510–550 nm, respectively. Images were acquired every 3 s, digitized and then analyzed using LAS AF 2.2.0 Live Data Mode software (Leica Microsystems, Germany). Data were expressed as F/Fmax where F is the increase of fluorescence after each single treatment and Fmax is the mean maximal change of fluorescence intensity upon addition of reagents. After background subtraction, the change in fluorescence (ΔF) was divided by the initial fluorescence (F0) to obtain a measure (ΔF/F0) that is proportional to the change in Ca^{2+} ($\Delta Ca^{2+} = \Delta F/F0$).

2.6. Fluorescence resonance energy transfer (FRET) acceptor bleaching method

The OX-1R/CB_1R molecular interaction was analyzed using the FRET acceptor photo-bleaching method. Briefly, after treatment, the cells were immunostained using goat anti-OX-1R and rabbit anti-CB_1R primary antibodies and respective secondary antibodies conjugated with Cy3 (donor) and Cy5 (acceptor), where the Cy3/Cy5 couple has a Förster distance of ~ 5 nm. The cells were excited sequentially for Cy5 and Cy3 and emission recorded with adequate advanced ultrafast filter wheels ensuring accurate imag-

ing (Leica Microsystems). The cells were photobleached and pre- and post-bleach images were captured simultaneously. The FRET efficiency was calculated by comparing donor Cy3 fluorescence intensity in the same sample, before and after destroying the acceptor Cy5 by photobleaching. If FRET was initially present, a resultant increase in donor fluorescence would occur following acceptor photobleaching. The FRET efficiency was calculated using the following formula: $E = 1 - I_{DA}/I_D$, wherein the intensity of Cy3 (donor) fluorescence was measured before (I_{DA}) and after (I_D) Cy5 photobleaching [19]. All experiments were performed in triplicate and data presented as means ± SD. Image frames were collected using the Leica digital microscope DMI6000 equipped with the appropriate filter wheels and the LAS AF FRET SE Wizard software. Control samples labeled with the donor (Cy3) and acceptor (Cy5) alone were used to verify that no bleed-through of acceptor fluorescence was present in the donor channel. In order to ensure that photobleaching per se does not perturb donor fluorescence, we measured FRET by omitting CB_1R primary antibody and bleaching Cy5 in samples labelled with OX-1R-Cy3 alone. The background value was subtracted from all samples.

2.7. Western blot analysis

ERK phosphorylation as well as OX-1R expression was assessed using western blot analysis. Briefly, mHypoE-N41 cells were lysed in a buffer solution (Tris HCl 50 mM, NaCl 150 mM, 1% Triton X-100, EDTA 2 mM, EGTA 5 mM, and protease inhibitors mixture) and protein concentrations were quantified using Lowry protein assay (Bio-Rad Laboratories). Twenty μg of protein were subjected to 10% polyacrylamide gel electrophoresis and finally, transferred to PVDF membranes. Membranes were blocked with non-fat dry powdered milk for 2 h and incubated overnight at 4 °C with ERK1/2 (1:1000; Cell Signaling), pERK1/2 Thr202/Tyr204 (1:1000; Cell Signaling), or goat anti-OX-1R antibody (1:500; Santa Cruz Biotechnology), followed by 2 h incubation with appropriate secondary antibody (Peroxidase labeled ECL). A monoclonal anti-β-actin antibody (1:4000; Sigma-Aldrich) was used as the reference protein expression. Detection was performed using chemiluminescence (Clarity ECL; Biorad). Images were analyzed on a ChemiDoc station with ImageJ software.

2.8. Immunoprecipitation

After treatment, the cells were lysed and protein concentrations were quantified as described above. One mg of cell lysate was used for the immunoprecipitation (IP) procedure using a Dynabeads Protein G Kit (Life Technology) following the manufacturer's instructions. Briefly, 10 mg of mouse anti-CB_1R antibody (Calbiochem) was used to immunoprecipitate all proteins bound to CB_1R. IP proteins were recovered by heating at 70 °C for 10 min through the captured bead/ProteinG/antigen complex. After loading on SDS-polyacrylamide (10%) gel, IP proteins were transferred to a PVDF membrane and then the membranes incubated with the primary polyclonal antibodies anti-CB_1R (1:500, Calbiochem) or anti-OX-1R (1:100, Santa Cruz) overnight at 4 °C. Finally, the membranes were exposed to the secondary antibody (Peroxidase labeled ECLTM) for 2 h at room temperature. Detection was performed using chemiluminescence (Clarity ECL; Biorad) and the images were analyzed on a ChemiDoc station as indicated above.

2.9. Lipid extraction and 2-AG measurement

After treatment, the cells (each data point contained 5×10^5 cells) and supernatants were homogenized in 50 mmol/L Tris·HCl, pH 7.5, in chloroform/methanol (1:2:1, vol/vol) containing 5 pmol of [^{2}H]$_5$-2-AG as internal standard, and analysed using liquid chromatography-atmospheric pressure chemical ionization-mass spectrometry (LC–MS) as previously described [20]. 2-AG levels were calculated on the basis of their peak area ratio (in the SIM mode) with the internal deuterated standard peak areas, and their amounts (pmol) were normalized per ml of cells plus medium.

2.10. Statistical analyses

Data are expressed as mean ± SEM or mean ± SD and were analyzed with GraphPad Prism 6 software, version 6.05 (GraphPad, Inc.). Statistical differences among treatments were determined by two-way ANOVA followed by post hoc Bonferroni tests for comparison among means.

3. Results

3.1. Simultaneous activation of OX-1R and CB_1R enhances $[Ca^{2+}]_i$ in mHypoE-N41 neurons

We and others reported the occurrence of a functional interaction between OX-1R and CB_1R in the brain [13–16,21]. Both these receptors belong to the GPCRs superfamily with differences in the type of G protein to which they couple, with CB_1R mainly associated to Gi/o [22,23], and OX-1R to Gq [2]. We therefore investigated the alteration of $[Ca^{2+}]_i$ induced by either CB_1R and OX-1R activation in mHypoE-N41 cells. Using immunocytochemical techniques, we confirmed in these cells the expression of both these receptors. CB_1R and OX-1R were constitutively expressed in mHypoE-N41 cells, often in the same cell department, as shown by the yellow colour in the merge of Fig. 1. Fluo-4AM, a cell-permeable Ca^{2+} indicator, was used to measure $[Ca^{2+}]_i$ in mHypoE-N41 cells after treatment with increasing concentrations of OX-A, which was previously reported to increase Ca^{2+} levels in primary neurons [24]. In this cell line, OX-A was able to induce a transient cytosolic Ca^{2+} peak with the maximum effect at 0.2 μM, whereas a very weak effect was observed at 0.3 μM possibly due to agonist-induced receptor desensitization (Fig. 2). This effect was prevented by SB334867 (10 μM), a selective OX-1R antagonist. No $[Ca^{2+}]_i$ modification was found at the concentration of 0.1 μM OX-A. As expected, the cytosolic Ca^{2+} levels were not significantly modified by treatement with different concentrations of ACEA, a CB_1R agonist (Fig. 2). In order to provide evidence for a synergistic role of OX-1R and CB_1R on $[Ca^{2+}]_i$, we then treated the cells with a sub-effective dose of OX-A (0.1 μM) in combination with ACEA (0.1 μM). As shown in Fig. 3, this resulted in the prolonged and strong increase of $[Ca^{2+}]_i$. This response was prevented by pre-incubation with both AM251 (0.5 μM), a CB_1R antagonist/inverse agonist, and SB334867 (10 μM). Taken together, these data suggest the possibility that a synergistic action occurs between OX-1R and CB_1R in the control of $[Ca^{2+}]_i$.

3.2. A physical interaction between OX-1R and CB_1R is induced by OX-A in mHypoE-N41 cells

It is generally believed that both CB_1R and OX-1R are able to form homo- and heteromeric complexes with one another as well as with other types of G-protein-coupled receptors [25]. Since CB_1R/OX-1R heterodimerization occurs in recombinant cells overexpressing both the receptors, and affect the pharmacology of both receptor types, we investigated in mHypoE-N41cells the formation of CB_1R/OX-1R heteromers and their putative effects on $[Ca^{2+}]_i$ elevation. The CB_1R/OX-1R physical interaction was determined by using a FRET approach based on acceptor photobleaching technique by recording the changes in the donor fluorescence [19]. We found that FRET efficiency was significantly higher in mHypoE-N41cells after 30 min treatment with OX-A (0.2 μM) compared to control cells (Fig. 4). This effect was prevented by SB334867
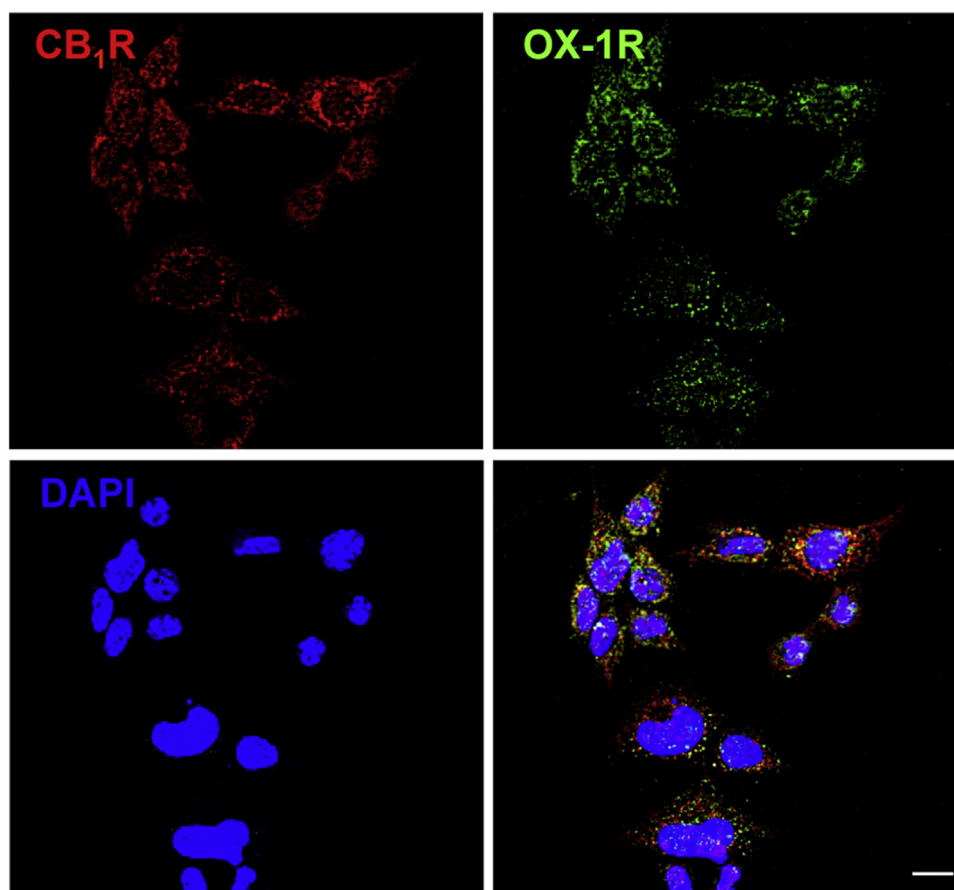
Fig. 1. Expression of OX-1R and CB$_1$R in mHypoE-N41 cells. Representative confocal images of the CB$_1$R (red signal) or OX-1R (green signal) immunocytochemical staining in mHypoE-N41 cells. Cell nuclei were counterstained with DAPI (blue signal). Scale bar:10 μm.

(10 μM). Besides, the FRET efficiency observed after treatment with either 0.1 μM OX-A or ACEA (0.1 μM and 0.2 μM) alone was not significantly different from the control cells. It is important to note, however, that an ineffective dose of OX-A (0.1 μM) in combination with ACEA (0.1 μM) was able to increase the donor fluorescence intensity after acceptor photobleaching, yielding a FRET efficiency similar to that observed with 0.2 μM OX-A alone. This enhanced FRET efficiency was prevented by both AM251 and SB334867. In order to further confirm the occurrence of OX-1R/CB$_1$R heteromers, we exploited the OX-1R/CB$_1$R co-immunoprecipitation assay in mHypoE-N41 cells treated with OX-A (0.1 μM) or ACEA (0.1 μM), alone or in combination. Similar to what observed with the FRET assay, either agonist per se was not able to produce OX-1R/CB$_1$R co-immunoprecipitation, an effect which was instead observed upon cell treatment with the combination of the two agonists (Fig. 5). As aspected, this effect was prevented by both SB334867 and AM251 (Fig. 5).

Taken together, these results are consistent with the hypothesis that in order to form OX-1R/CB$_1$R heteromers a combination of agonists of either receptor at subeffective concentrations is needed. They also suggest that an effective concentration of an OX-1R, but not of a CB$_1$R, agonist may induce heteromerization.

3.3. OX-A-induced 2-AG biosynthesis is enhanced by ACEA

It well known that OX-1R, coupled to Gq proteins, induces the activation of PLCβ with consequent production of IP3 and DAG, the DAGLα substrate and precursor of 2-AG, the most abundant endocannabinoid in the brain [26]. Previous studies from our and other laboratories have demonstrated that OX-A triggers the biosynthesis of 2-AG both in vivo and in vitro [14,15,17,27]. Here we investigated if OX-A-induced 2-AG biosynthesis also occurs in mHypoE-N41 cells and if this was affected by the formation of CB$_1$R/OX-1R heteromers. With this purpose, 2-AG levels were analyzed in cells treated with OX-A alone (0.2 μM) or with OX-A (0.1 μM) in combination with ACEA (0.1 μM). As shown in Table 1, 2-AG levels, detected using LC–MS, were significantly increased in cells exposed to 0.2 μM OX-A. The same effect was induced by OX-A (0.1 μM) in combination with ACEA (0.1 μM), in a manner sensitive to both SB334867 and AM251. It is important to note that ACEA (0.1 μM) alone was unable to induce 2-AG biosynthesis, and that the elevation of 2-AG levels induced by either OX-A 0.2 μM alone or OX-A (0.1 μM) + ACEA (0.1 μM) was erased by co-incubation with the DAGLα inhibitor O-7460 [28].

3.4. OX-A-and ACEA synergize at inducing ERK phosphorylation

It has been reported that CB$_1$R/OX-1R heteromerization induces downstream signaling alterations for both receptors [16]. Since extracellular signal–regulated kinase1/2 (ERK1/2) signaling is one of the main pathways downstream to both OX-1R and CB$_1$R [8,29–32], we investigated if treatment with OX-A alone (0.2 μM) or OX-A (0.1 μM) in combination with ACEA (0.1 μM) induces an alteration in ERK1/2 phosphorylation. As shown in Fig. 6, a 30 min treatment with OX-A (0.2 μM) or ACEA (0.2 μM), as well as OX-A (0.1 μM) + ACEA (0.1 μM) induced a strong increase of ERK phosphorylation, as assessed by WB analysis, in a manner sensitive to both SB334867 (10 μM) and AM251 (0.5 μM). The effect of OX-A (0.1 μM) + ACEA (0.1 μM) was stronger than the effect of OX-A (0.2 μM) or ACEA (0.2 μM) alone.
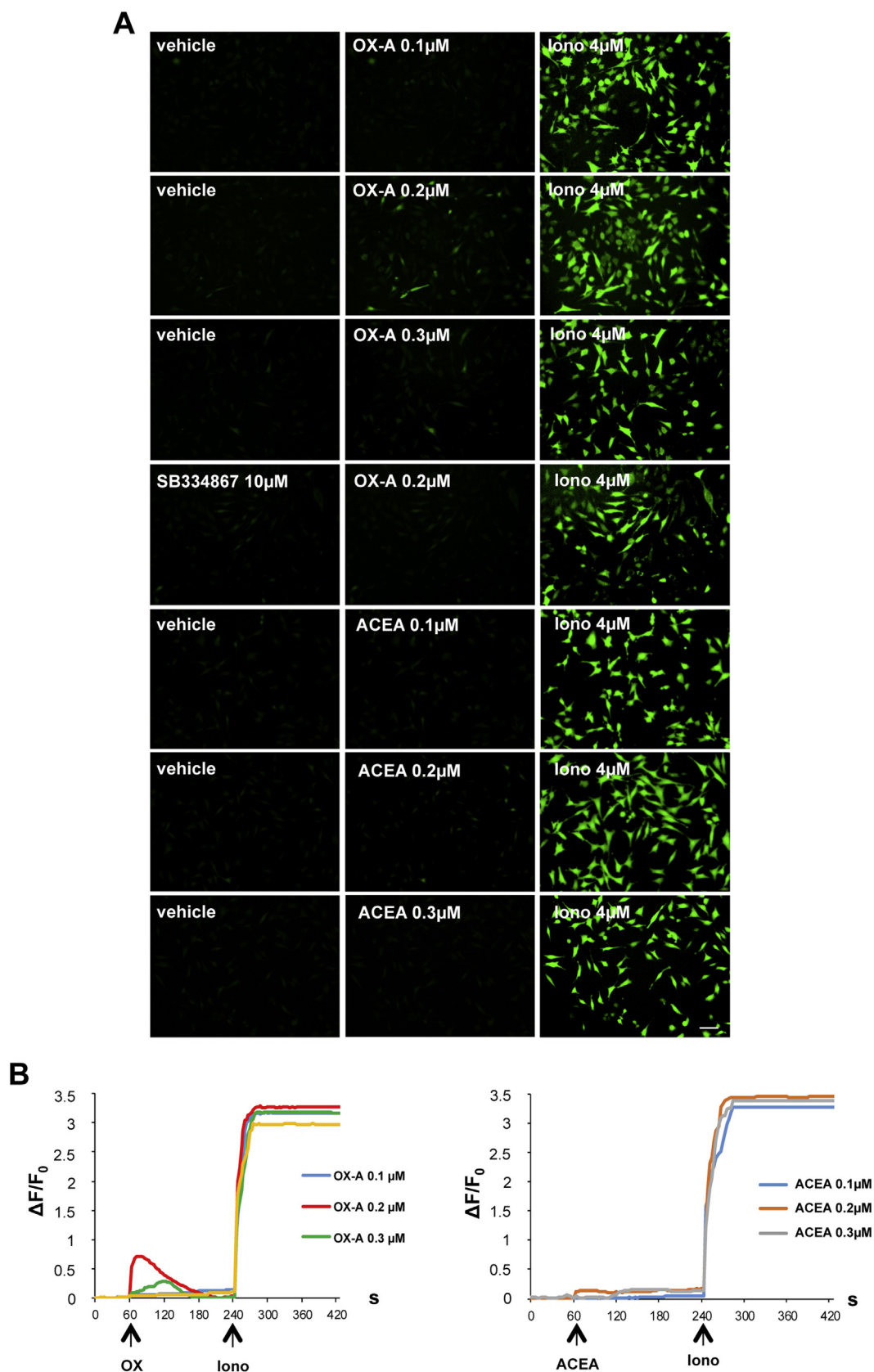
Fig. 2. Effect of OX-A or ACEA on intracellular Ca^{2+}. A) Representative micrographs of Ca^{2+} accumulation in Fluo-4AM- loaded mHypoE-N41 cells treated with different concentrations of OX-A or ACEA. The Fluo-4AM-loaded cells were also exposed to SB334867 (10 μM) 15 min before OX-A (0.2 μM) treatment. Untreated and OX-A-treated cells were also exposed to ionomycin (4 μM). Images, collected continuosly for 420 s, were analyzed to quantify the mean fluorescence of individual cells using Metamorph Imaging Software (Leica MetaMorph AF). Scale bar: 20 μm. B) Representative traces of the Ca^{2+} response expressed as $\Delta F/F0$ intensity of cells treated with OX-A or ACEA and with SB334867. Arrows indicate when OX-A or ionomycin (4 μM) were added to the cells.
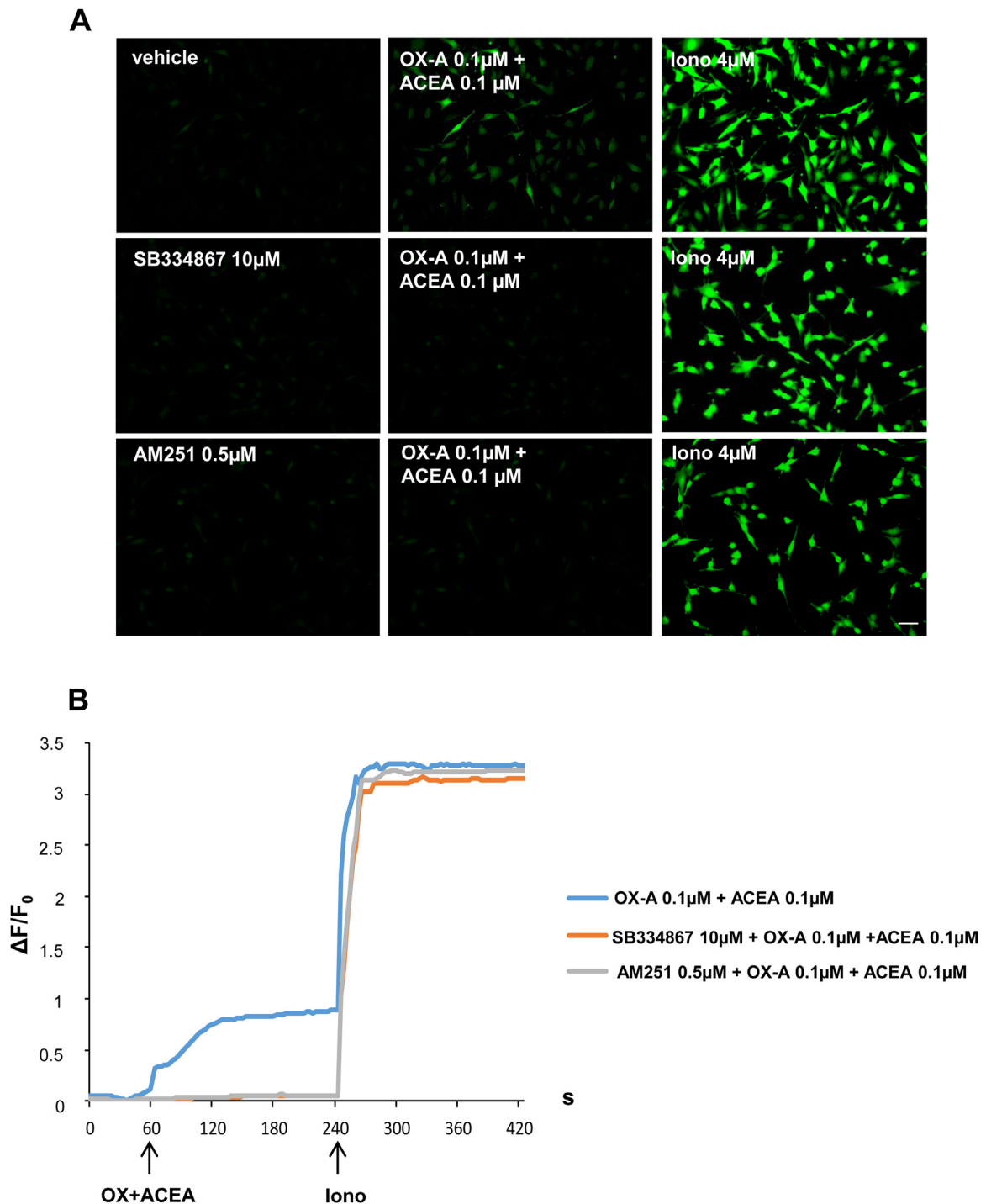
Fig. 3. OX-A and ACEA exert a synergistic potentiation on intracellular Ca^{2+} at doses per se ineffective. A) Representative micrographs of Ca^{2+} accumulation in Fluo-4AM-loaded mHypoE-N41 cells treated with the combination of ACEA ($0.1\,\mu$M) and OX-A ($0.1\,\mu$M) in the absence or presence of SB334867 ($10\,\mu$M, 15 min before ACEA/OX-A treatment) or AM251 ($0.5\,\mu$M, 15 min before ACEA/OX-A treatment). Untreated and ACEA/OX-A-treated cells were also exposed to ionomycin ($4\,\mu$M). Images were collected and analyzed as indicated above. Scale bar: $20\,\mu$m. B) Representative traces of the Ca^{2+} response expressed as $\Delta F/F0$ intensity in cells treated as indicated in A. Arrows indicate when ACEA in combination with OX-A, or ionomycin ($4\,\mu$M), were added to the cells.

4. Discussion

The findings of the present study are in agreement with previous in vitro FRET studies which described the occurrence of OX-1R/CB_1R heteromerization when these two receptors are heterologously expressed in the same cell [3,9–12]. However, here we analyzed native hypothalamic NPY/AgRP neurons, which express constitutively both OX-1R and CB_1R. This situation represents more

appropriately the in vivo hypothalamic circuits involved in the control of important physiological function, such as food intake [17]. One of the most frequent consequences of OX-1R activation is the elevation of $[Ca^{2+}]_i$, as found in many recombinant systems as well as in neurons [2,3,33–37]. This response was originally accounted for by the canonical pathway of $Gq \rightarrow PLC \rightarrow$ inositol-1,4,5- trisphosphate (IP3) $\rightarrow Ca^{2+}$ release from the endoplasmic reticulum. However, an unexpected discovery was that this
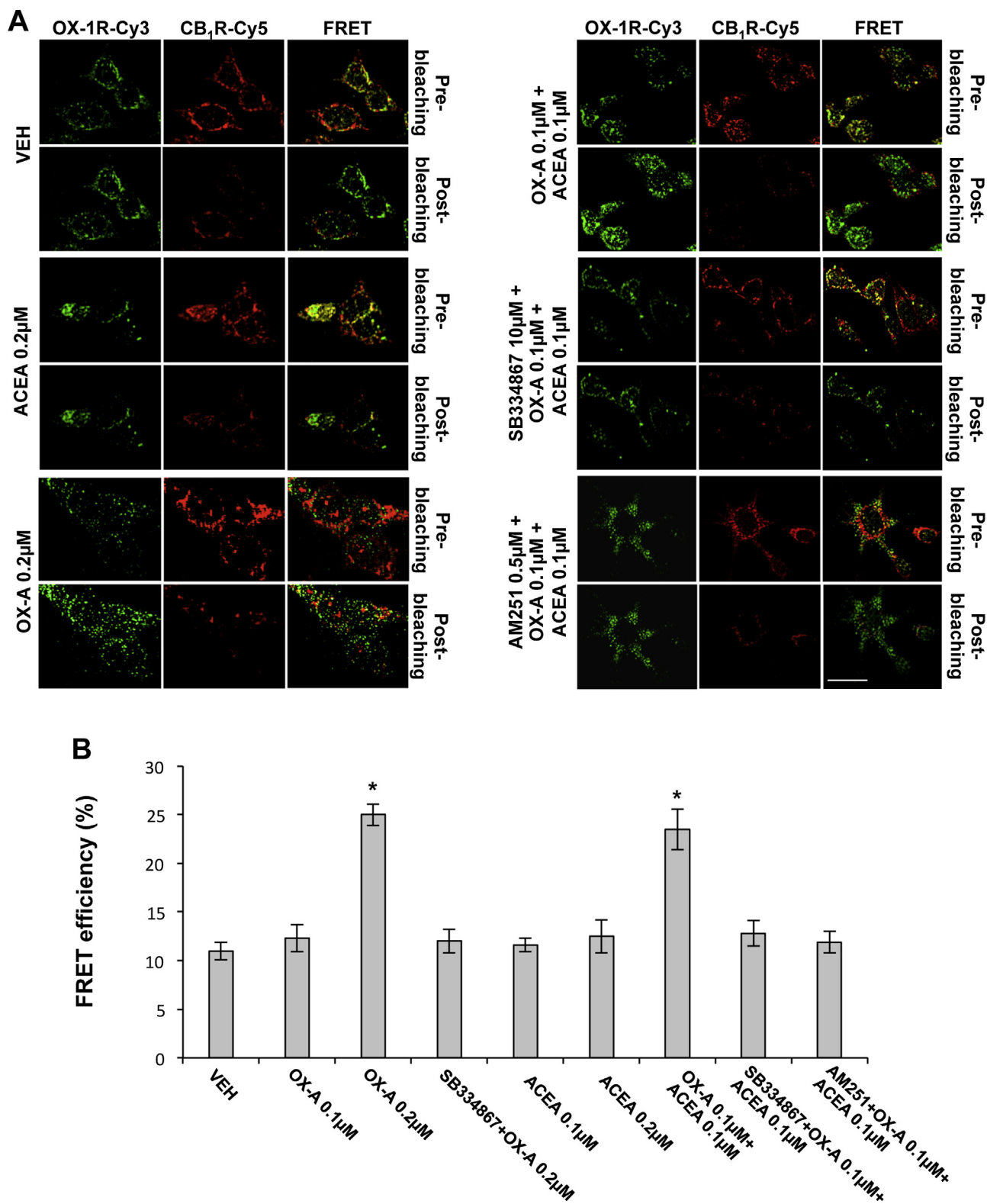
Fig. 4. Fluorescence resonance energy transfer (FRET) efficiency of OX-1R or CB$_1$R in mHypoE-N41 cells. A) Representative images of OX-1R/CB$_1$R FRET assay in untreated cells or cells treated with ACEA (0.2 μM for 30 min) or OX-A (0.2 μM for 30 min). In some experiments cells were treated with the combination of OXA (0.1 μM) and ACEA (0.1 μM), in the absence or presence of SB334867 (10 μM, 15 min before OX-A/ACEA treatment) or AM 251 (0.5 μM, 15 min before OX-A/ACEA treatment). B) Mean of OX-1R/CB$_1$R FRET efficiency in untreated cells or cells treated with OX-A (0.2 μM for 30 min), in the absence or presence of SB334867 (10 μM, 15 min before OX-A treatment) or AM 251 (0.5 μM, 15 min before OX-A treatment). OX-1R/CB$_1$R FRET efficiency was also measured in cells exposed to ACEA (0.2 μM), to a mix of OX-A (0.1 μM) and ACEA (0.1 μM), with or without SB334867 (10 μM, 15 min before OX-A/ACEA treatment) or AM251 (0.5 μM, 15 min before OX-A/ACEA treatment). Data are means ± SD of at least three separate experiments, each performed in triplicate. Statistical analysis was performed by two-way ANOVA followed by the Bonferroni post-hoc test. **p < 0.001 vs vehicle-treated cells.

IP:CB$_1$R

Fig. 5. Co-immunoprecipitation of OX-1R and CB$_1$R from mHypoE-N41 cells. Cells were treated with OX-A (0.1 μM for 30 min) in the absence or presence of ACEA (0.1 μM for 30 min). In some experiments, cells were exposed to the combination of OX-A (0.1 μM) and ACEA (0.1 μM), in the absence or presence of SB334867 (10 μM, 15 min before OX-A/ACEA treatment) or AM251 (0.5 μM, 15 min before OX-A/ACEA treatment). After treatment, cells, prepared as described in Materials and methods, were processed for immunoprecipitation with an anti-CB$_1$R antibody. IP proteins were analyzed by immunoblotting with anti-CB$_1$R or OX-1R antibodies. Fold data represent the means ± SD of at least three separate experiments, each performed in triplicate. Statistical analysis was performed by two-way ANOVA followed by the Bonferroni post-hoc test. *p < 0.01 vs vehicle-treated cells.
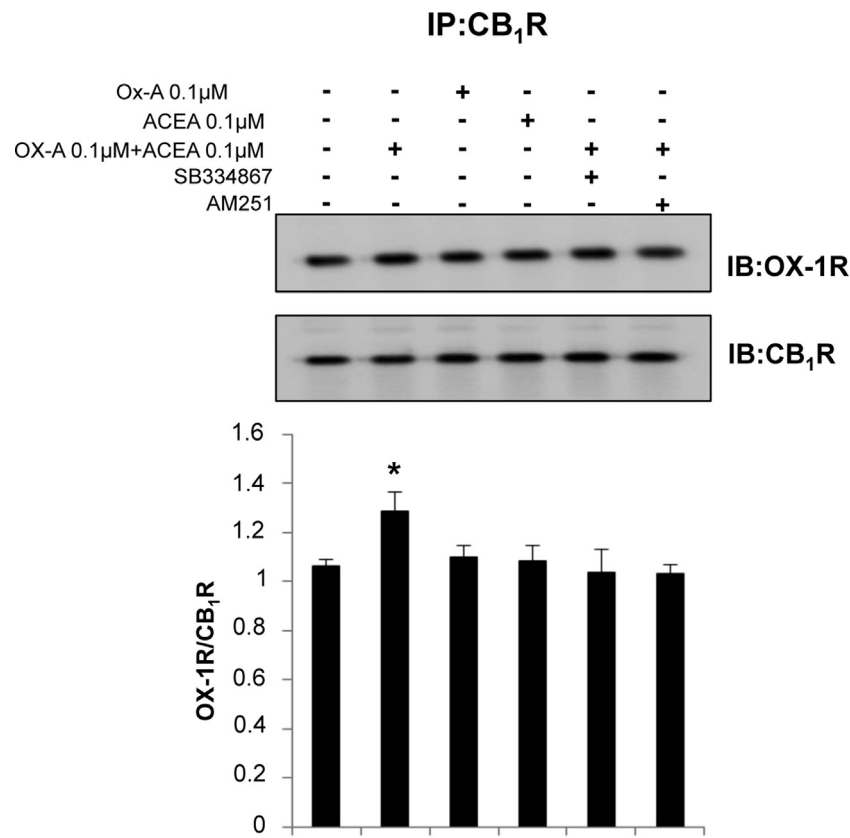
Table 1
2-AG levels in mHypoE-N41cells.

Treatment	2-AG (pmol/ml)
Untreated	3.2 ± 1.8
OX-A (0.1 μM)	4.0 ± 0.7
ACEA (0.1 μM)	2.8 ± 0.7
OX-A (0.1 μM)/ACEA (0.1 μM)	200 ± 40***
OX-A (0.1 μM)/ACEA (0.1 μM)/SB334867	4.5 ± 0.4 (***)
OX-A (0.1 μM)/ACEA (0.1 μM)/AM251	2.6 ± 0.5 (***)
OX-A (0.2 μM)	270 ± 60***
OX-A (0.2 μM)/O-7460	6.7 ± 1.8°°°
OX-A(0.1 μM)/ACEA (0.1 μM)/O-7460	5.6 ± 0.5 (***)
SB334867	3.4 ± 1.4
AM251	4.2 ± 1.0
O-7460	6.1 ± 1.5

Endogenous levels of 2-AG were quantified by LC–MS in mHypoE-N41 cells treated with OX-A (0.1 μM; 30 min) in the absence or presence of ACEA (0.1 μM). In other experiments, the cells were treated with OX-A (0.1 μM)/ACEA (0.1 μM) after 15 min pre-exposure to SB334867 (10 μM) or AM251 (0.5 μM) or O-7460 (10 μM, a selective DAGLα inhibitor). Data from untreated cells as well as from cells treated with 0.1 μM ACEA, 0.2 μM OX-A, SB334867 or AM251 are also reported. 2-AG levels were normalized per ml of cells + medium. Each sample contained 5×10^5 cells. Results represent means ± SEM of three separate experiments, and were compared by using two-way ANOVA followed by the Bonferroni's test. ***p < 0.0001 vs vehicle-treated cells; (***)p < 0.0001 vs OX-A/ACEA treated cells; °°° p < 0.0001 vs. OX-A treated cells.

response required extracellular Ca^{2+} influx through non-selective calcium operated channels (i.e. voltage-gated Ca^{2+} channels, a reverse-acting Na$^+$/Ca^{2+} exchanger, store-operated Ca^{2+} channels or non-selective cation channels; reviewed in [3] and [37]). This

response was identified as the major mediator of orexin-induced depolarization in CNS neurons [3,32,37–42] and is different from that seen in the canonical PLC–Ca^{2+} release pathway since: *i*) it is a very early response to OX-A/OX-1R binding and is not secondary to Ca^{2+} store release (store-operated Ca^{2+} influx; reviewed in [43]); *ii*) it does not require IP3 [3,11,32,37,44–46]. Here, we tested OX-1R and CB$_1$R functionality in terms of their effect on [Ca^{2+}]$_i$ and how such effects are influenced by either simultaneous or separate activation of the receptors. An increase of [Ca^{2+}]$_i$ occured after cell treatment with a combination of OX-A and ACEA at the doses that produced no effect per se. This effect was stronger than the similar effect observed with the optimal concentration of OX-A and was blocked by pretreatment of cells with the antagonists SB334867 and AM251, suggesting a synergistic OX-1R/CB$_1$R interaction in mHypoE-N41 native cells. This functional interaction is likely due to CB$_1$R and OX-1R heteromerization, as directly shown here by using a FRET assay. Indeed, using the same experimental conditions as with the [Ca^{2+}]$_i$ assay, we found an increase of FRET efficiency, and detected OX-1R and CB$_1$R co-immunoprecipitation, after simultaneous stimulation of OX-1R and CB$_1$R. These effects were blunted in cells pretreated with either SB334867 or AM251, indicating that the correct functionality of both OX-1R and CB$_1$R is crucial for their heteromerization.

It has been proposed that OX-1R and CB$_1$R form heteromeric complexes that affect trafficking of OX-1R and potentiate CB$_1$R signaling. Moreover, it has been shown, in CHO cells overexpressing the recombinant receptors, that OX-1R activation releases 2-AG, which then acts as a potent paracrine messenger stimulating CB$_1$R on neighboring cells [3,9–12]. Our findings not only
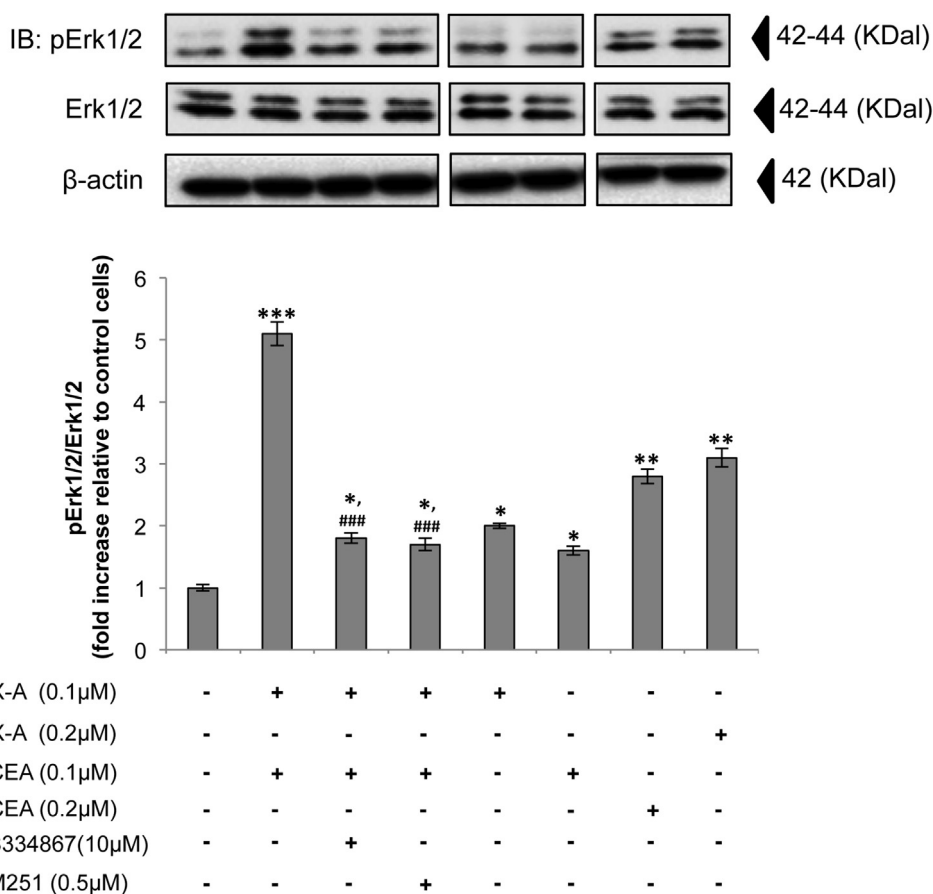
Fig. 6. Co-incubation of mHypoE-N41 cells with ACEA and OX-A enhances ERK phosphorylation. Representative immunoblots of ERK1/2 phosphorylation in cells exposed to OX-A (0.1 or 0.2 μM, 30 min), ACEA (0.1 or 0.2 μM, 30 min) or a mix of OX-A (0.1 μM) and ACEA (0.1 μM), in the absence or presence of SB334867 (10 μM, 15 min before OX-A/ACEA treatment) or AM251 (0.5 μM, 15 min before OX-A/ACEA treatment). Fold data represent the means ± SEM of at least three separate experiments, each performed in triplicate and normalized to vehicle-treated cells. Statistical analysis was performed by two-way ANOVA followed by the Bonferroni post-hoc test. *$p < 0.05$, **$p < 0.005$, ***$p < 0.0005$ vs vehicle-treated cells; ###$p < 0.0005$ vs OX-A/ACEA-treated cells.

reveal the formation of OX-1R/CB$_1$R heteromeric complex in a more physiologically relevant neuronal model, but also identify Gq(OX-1R)-PLC-DAGL-dependent 2-AG production as a potentially important contributor to the OX-1R/CB$_1$R synergism, which, therefore, occurs at the level of both the physical interaction between the two receptors and their downstream signals. In fact, our data show that: i) OX-A-induced, and DAGL-mediated, biosynthesis of 2-AG is enhanced by ACEA; ii) a similar intensity of signal outcomes, in terms of FRET efficiency, [Ca^{2+}]$_i$ elevation, ERK phosphorylation and 2-AG biosynthesis, is achieved in cells upon incubation with either OX-A alone, at an efficacious concentration (0.2 μM), or OX-A + ACEA at concentrations otherwise ineffective per se (0.1 μM). These results are of special relevance to previous in vivo findings showing that Gq(OX-1R)-PLC-DAGL-dependent 2-AG production occurs in hypothalamic areas regulating energy homeostasis [15–17] or in extra-hypothalamic areas, i.e. the PAG and the VTA, involved in the control of nociception [13,14] or in reward and drug seeking behaviors [47], respectively. The proximity of the two receptors in a heteromer might represent an effective mechanism to potentiate common downstream signals, i.e. ERK1/2 activity, when the single basal OX-A and 2-AG levels are not sufficient alone, particularly as OX-1R efficiently activates 2-AG production, and also this effect appeared here to be amplified by the heteromerization of the two receptors.

In agreement with its physiological function, OX-A in the hypothalamus exhibits strong diurnal fluctuations, with peaks occurring during sleep to wake transitions, arousal and appetite

[48]. OX-A up-regulation is paralleled by elevation of 2-AG levels in the same area in rodents [15,17]. Starting from the present data, it is tempting to suggest that the occurrence of OX-1R/CB$_1$R heteromerization, together with the reciprocal fluctuations of OX-A and 2-AG levels in the brain, lead to the amplification of downstream cells signals as well as endocannabinoid levels, during different physiological or pathological states.

Conflict of interest

All authors declare no conflict of interest.

References

[1] G. Turu, L. Hunyady, Signal transduction of the CB1 cannabinoid receptor, J. Mol. Endocrinol. 44 (2010) 75–85.
[2] T. Sakurai, A. Amemiya, M. Ishii, I. Matsuzaki, R.M. Chemelli, H. Tanaka, et al., Orexins and orexin receptors: a family of hypothalamic neuropeptides and g protein-coupled receptors that regulate feeding behavior, Cell 92 (1998) 573–585.
[3] J.P. Kukkonen, C.S. Leonard, Orexin/hypocretin receptor signalling cascades, Br. J. Pharmacol. 171 (2014) 314–331.
[4] L. de Lecea, T.S. Kilduff, C. Peyron, X. Gao, P.E. Foye, P.E. Danielson, et al., The hypocretins: hypothalamus-specific peptides with neuroexcitatory activity, Proc. Natl. Acad. Sci. U. S. A. 95 (1998) 322–327.
[5] C. Peyron, D.K. Tighe, A.N. Van Den Pol, L. De Lecea, H.C. Heller, J.G. Sutcliffe, T.S. Kilduff, Neurons containing hypocretin (orexin) project to multiple neuronal systems, J. Neurosci. 18 (1998) 9996–10015.
[6] T. Sakurai, The neural circuit of orexin (hypocretin): maintaining sleep and wakefulness, Nat. Rev. Neurosci. 8 (2007) 171–181.

[7] N. Tsujino, T. Sakurai, Orexin/hypocretin: a neuropeptide at the interface of sleep energy homeostasis, and reward system, Pharmacology 61 (2009) 162–176.

[8] S. Hilairet, M. Bouaboula, D. Carrière, G. Le Fur, P. Casellas, Hypersensitization of the Orexin 1 receptor by the CB1 receptor: evidence for cross-talk blocked by the specific CB1 antagonist, SR141716, J. Biol. Chem. 278 (2003) 23731–23737.

[9] J. Ellis, J.D. Pediani, M. Canals, S. Milasta, G. Milligan, Orexin-1 receptor-cannabinoid CB1 receptor heterodimerization results in both ligand-dependent and -independent coordinated alterations of receptor localization and function, J. Biol. Chem. 281 (2006) 38812–38824.

[10] R.J. Ward, J.D. Pediani, G. Milligan, Ligand-induced internalization of the orexin OX(1) and cannabinoid CB(1) receptors assessed via N-terminal SNAP and CLIP-tagging, Br. J. Pharmacol. 162 (2011) 1439–1452.

[11] P.M. Turunen, M.H. Jäntti, J.P. Kukkonen, OX1 orexin/hypocretin receptor signaling through arachidonic acid and endocannabinoid release, Mol. Pharmacol. 82 (2012) 156–167.

[12] M.H. Jäntti, J. Putula, P.M. Turunen, J. Näsman, S. Reijonen, C. Lindqvist, J.P. Kukkonen, Autocrine endocannabinoid signaling through CB1 receptors potentiates OX1 orexin receptor signaling, Mol. Pharmacol. 83 (2013) 621–632.

[13] Y.C. Ho, H.J. Lee, L.W. Tung, Y.Y. Liao, S.Y. Fu, S.F. Teng, H.T. Liao, K. Mackie, L.C. Chiou, Activation of orexin 1 receptors in the periaqueductal gray of male rats leads to antinociception via retrograde endocannabinoid (2-arachidonoylglycerol)-induced disinhibition, J. Neurosci. 31 (2011) 14600–14610.

[14] L. Cristino, L. Luongo, R. Imperatore, S. Boccella, T. Becker, G. Morello, F. Piscitelli, G. Busetto, S. Maione, V. Di Marzo, Orexin-A and endocannabinoid activation of the descending antinociceptive pathway underlies altered pain perception in leptin signaling deficiency, Neuropsychopharmacology 41 (2016) 508–520.

[15] L. Cristino, G. Busetto, R. Imperatore, I. Ferrandino, L. Palomba, C. Silvestri, S. Petrosino, P. Orlando, M. Bentivoglio, K. Mackie, V. Di Marzo, Obesity-driven synaptic remodeling affects endocannabinoid control of orexinergic neurons, Proc. Natl. Acad. Sci. U. S. A. 110 (2013) E2229–E2238.

[16] A. Flores, R. Maldonado, F. Berrendero, Cannabinoid-hypocretin cross-talk in the central nervous system: what we know so far, Front. Neurosci. 7 (2013) 256.

[17] G. Morello, R. Imperatore, L. Palomba, C. Finelli, G. Labruna, F. Pasanisi, L. Sacchetti, L. Buono, F. Piscitelli, P. Orlando, V. Di Marzo, L. Cristino, Orexin-A represses satiety-inducing POMC neurons and contributes to obesity via stimulation of endocannabinoid signalling, Proc. Natl. Acad. Sci. U. S. A. 113 (2016) 4759–4764.

[18] V. Di Marzo, S.K. Goparaju, L. Wang, J. Liu, S. Bátkai, Z. Járai, F. Fezza, G.I. Miura, R.D. Palmiter, T. Sugiura, G. Kunos, Leptin-regulated endocannabinoids are involved in maintaining food intake, Nature 410 (2001) 822–825.

[19] H.C. Ishikawa-Ankerhold, R. Ankerhold, G.P.C. Drummen, Advanced fluorescence microscopy techniques—FRAP, FLIP FLAP, FRET and FLIM, Molecules 17 (2012) 4047–4132.

[20] S. Petrosino, A. Schiano Moriello, S. Cerrato, M. Fusco, A. Puigdemont, L. De Petrocellis, V. Di Marzo, The anti-inflammatory mediator palmitoylethanolamide enhances the levels of 2-arachidonoyl-glycerol and potentiates its actions at transient receptor potential vanilloid type-1 channels, Br. J. Pharmacol. 173 (2015) 1154–1162.

[21] S. Haj-Dahmane, R.Y. Shen, The wake-promoting peptide orexin-B inhibits glutamatergic transmission to dorsal raphe nucleus serotonin neurons through retrograde endocannabinoid signaling, J. Neurosci. 25 (2005) 896–905.

[22] A.C. Howlett, J.M. Qualy, L.L. Khachatrian, Involvement of Gi in the inhibition of adenylate cyclase by cannabimimetic drugs, Mol. Pharmacol. 29 (1986) 307–313.

[23] D.M. Slipetz, G.P. O'Neill, L. Favreau, C. Dufresne, M. Gallant, Y. Gareau, D. Guay, M. Labelle, K.M. Metters, Activation of the human peripheral cannabinoid receptor results in inhibition of adenylyl cyclase, Mol. Pharmacol. 48 (1995) 352–361.

[24] W.N. Wu, P.F. Wu, J. Zhou, X.L. Guan, Z. Zhang, Y.J. Yang, L.H. Long, N. Xie, J.G. Chen, F. Wang, Orexin-A activates hypothalamic AMP-activated protein kinase signaling through a Ca^2+-dependent mechanism involving voltage-gated L-type calcium channel, Mol. Pharmacol. 84 (2013) 876–887.

[25] M.H. Jäntti, I. Mandrika, J.P. Kukkonen, Human orexin/hypocretin receptors form constitutive homo- and heteromeric complexes with each other and with human CB1 cannabinoid receptors, Biochem. Biophys. Res. Commun. 445 (2014) 486–490.

[26] J. Putula, T. Pihlajamaa, J.P. Kukkonen, Calcium affects OX1 orexin (hypocretin) receptor responses by modifying both orexin binding and the signal transduction machinery, Br. J. Pharmacol. 171 (2014) 5816–5828.

[27] P.M. Turunen, M.E. Ekholm, P. Somerharju, P.J. Kukkonen, Arachidonic acid release mediated by OX1 orexin receptors, Br. J. Pharmacol. 159 (2010) 212–221.

[28] T. Bisogno, A. Mahadevan, R. Coccurello, J.W. Chang, M. Allarà, Y. Chen, G. Giacovazzo, A. Lichtman, B. Cravatt, A. Moles, V. Di Marzo, A novel fluorophosphonate inhibitor of the biosynthesis of the endocannabinoid 2-arachidonoylglycerol with potential anti-obesity effects, Br. J. Pharmacol. 169 (2013) 784–793.

[29] S. Milasta, N.A. Evans, L. Ormiston, S. Wilson, R.J. Lefkowitz, G. Milligan, The sustainability of interactions between the orexin-1 receptor and β-arrestin-2 is defined by a single C-terminal cluster of hydroxy amino acids and modulates the kinetics of ERK MAPK regulation, Biochem. J. 387 (2005) 573–584.

[30] S. Ammoun, L. Johansson, M.E. Ekholm, T. Holmqvist, A.S. Danis, L. Korhonen, O.A. Sergeeva, H.L. Haas, K.E. Åkerman, J.P. Kukkonen, OX1 orexin receptors activate extracellular signal-regulated kinase (ERK) in CHO cells via multiple mechanisms: the role of Ca^{2+} influx in OX1 receptor signaling, Mol. Endocrinol. 20 (2006) 80–99.

[31] S. Ammoun, D. Lindholm, H. Wootz, K.E. Åkerman, J.P. Kukkonen, Gprotein-coupled ox1 orexin/hcrtr-1 hypocretin receptors induce caspase-7 3 dependent and -independent cell death through p38 mitogen-/stress-activated protein kinase, J. Biol. Chem. 281 (2006) 834–842.

[32] J.P. Kukkonen, Physiology of the orexinergic/hypocretinergic system: a revisit in 2012, Am. J. Physiol. Cell Physiol. 304 (2013) C2–C32.

[33] D. Smart, J.C. Jerman, S.J. Brough, S.L. Rushton, P.R. Murdock, F. Jewitt, N.A. Elshourbagy, C.E. Ellis, D.N. Middlemiss, F. Brown, Characterization of recombinant human orexin receptor pharmacology in a Chinese hamster ovary cell-line using FLIPR, Br. J. Pharmacol. 128 (1999) 1–3.

[34] P.E. Lund, R. Shariatmadari, A. Uustare, M. Detheux, M. Parmentier, J.P. Kukkonen, K.E. Akerman, The orexin OX1 receptor activates a novel Ca^{2+} influx pathway necessary for coupling to phospholipase C, J. Biol. Chem. 275 (2000) 30806–30812.

[35] T. Holmqvist, L. Johansson, M. Ostman, S. Ammoun, K.E. Akerman, J.P. Kukkonen, OX1 orexin receptors couple to adenylyl cyclase regulation via multiple mechanisms, J. Biol. Chem. 280 (2005) 6570–6579.

[36] J. Putula, P.M. Turunen, L. Johansson, J. Näsman, R. Ra, L. Korhonen, J.P. Kukkonen, Orexin/hypocretin receptor chimaeras reveal structural features important for orexin peptide distinction, FEBS Lett. 585 (2011) 1368–1374.

[37] C.S. Leonard, J.P. Kukkonen, Orexin/hypocretin receptor signalling: a functional perspective, Br. J. Pharmacol. 171 (2014) 294–313.

[38] R.E. Brown, O.A. Sergeeva, K.S. Eriksson, H.L. Haas, Convergent excitation of dorsal raphe serotonin neurons by multiple arousal systems (orexin/hypocretin, histamine and noradrenaline), J. Neurosci. 22 (2002) 8850–8859.

[39] S. Burlet, C.J. Tyler, C.S. Leonard, Direct and indirect excitation of laterodorsal tegmental neurons by hypocretin/orexin peptides: implications for wakefulness and narcolepsy, J. Neurosci. 22 (2002) 2862–2872.

[40] R.J. Liu, A.N. van den Pol, G.K. Aghajanian, Hypocretins (orexins) regulate serotonin neurons in the dorsal raphe nucleus by excitatory direct and inhibitory indirect actions, J. Neurosci. 22 (2002) 9453–9464.

[41] B. Yang, A.V. Ferguson, Orexin-A depolarizes dissociated rat area postrema neurons through activation of a nonselective cationic conductance, J. Neurosci. 22 (2002) 6303–6308.

[42] A.N. van den Pol, P.K. Ghosh, R.J. Liu, Y. Li, G.K. Aghajanian, X.B. Gao, Hypocretin (orexin) enhances neuron activity and cell synchrony in developing mouse GFP-expressing locus coeruleus, J. Physiol. 541 (2002) 169–185.

[43] V. Konieczny, M.V. Keebler, C.W. Taylor, Spatial organization of intracellular Ca2+ signals, Semin. Cell Dev. Biol. 23 (2012) 172–180.

[44] J.P. Kukkonen, K.E.O. Åkerman, Orexin receptors couple to Ca2+ channels different from store-operated Ca2+ channels, Neuroreport 12 (2001) 2017–2020.

[45] M.E. Ekholm, L. Johansson, J.P. Kukkonen, IP(3)-independent signalling of OX(1) orexin/hypocretin receptors to $Ca^{(2+)}$ influx and ERK, Biochem. Biophys. Res. Commun. 353 (2007) 475–480.

[46] L. Johansson, M.E. Ekholm, J.P. Kukkonen, Regulation of OX(1) orexin/hypocretin receptor-coupling to phospholipase C by $Ca^{(2+)}$ influx, Br. J. Pharmacol. 150 (2007) 97–104.

[47] A. Flores, R. Saravia, R. Maldonado, F. Berrendero, Orexins and fear: implications for the treatment of anxiety disorders, Trends Neurosci. 38 (2015) 550–559.

[48] Y. Yoshida, N. Fujiki, T. Nakajima, B. Ripley, H. Matsumura, H. Yoneda, E. Mignot, S. Nishino, Fluctuation of extracellular hypocretin-1 (orexin A) levels in the rat in relation to the light-dark cycle and sleep-wake activities, Eur. J. Neurosci. 14 (2001) 1075–1081.